

## Measurements of cross sections and analyzing powers for the inclusive $pp \rightarrow pn\pi^+$ reaction at 400 and 450 MeV

W. R. Falk

*Physics Department, University of Manitoba, Winnipeg, Manitoba, Canada*

E. G. Auld, G. Giles, G. Jones, G. J. Lolos,\* and W. Ziegler

*Physics Department, University of British Columbia, Vancouver, British Columbia, Canada*

P. L. Walden

*TRIUMF, Vancouver, British Columbia, Canada*

(Received 1 July 1985)

Single arm spectrometer measurements of the differential cross sections and analyzing powers of the  $pp \rightarrow pn\pi^+$  reaction have been performed at 400 and 450 MeV incident proton energy. The measurements covering an angular range from  $46^\circ$  to  $90^\circ$  (lab) spanned pion energies corresponding to production of the np system with relative energies between 0 and 30 MeV, a region where the influence of the np final state interaction is particularly important. The trend of the measured analyzing power is very similar to that of the  $pp \rightarrow d\pi^+$  reaction, and is well explained by calculations that use this latter data as input. Dominance of the triplet pn final state is implied by these results.

### I. INTRODUCTION

Much interest continues to be focused on the fundamental  $NN \rightarrow NN\pi$  pion production reactions at intermediate energies because of their importance to our understanding of the NN interaction. Extensive experimental and theoretical studies of the  $pp \rightarrow d\pi^+$  reaction from 300 to 800 MeV have been pursued in recent years.<sup>1-3</sup> At the present time the differential cross sections and analyzing power are quite well established over this whole energy region. Spin correlation experiments have also, although to a more limited extent, been carried out at a number of laboratories.<sup>2</sup> The experimental situation concerning pion production leading to three-particle final states is, however, much less clear. A number of measurements of the  $pp \rightarrow pn\pi^+$  breakup reaction have been carried out in kinematically complete experiments over the energy range 510–800 MeV.<sup>4-7</sup> In general, these experiments explored the regions of phase space where effects of the  $\Delta^{++}$  resonance would be enhanced. Very little data exist, however, for regions of phase space of low relative np energy, where final state np interactions are important. In those cases where the region of low relative np energy was included (such as those of Rev. 7), a strong enhancement due to final state interactions (FSI's) was reported.

Part of our current interest in the  $pp \rightarrow pn\pi^+$  reaction was stimulated by the recent observations concerning the enhanced probabilities of pion absorption on isoscalar ( $S=1$ ) nucleon pairs, compared to absorption on isovector ( $S=0$ ) nucleon pairs.<sup>8-10</sup> Such observations arose from comparisons of the  ${}^3\text{He}(\pi^+, 2p)p$  and  ${}^3\text{He}(\pi^-, pn)n$  reaction cross sections. In the  $pp \rightarrow pn\pi^+$  reaction the pn final system can involve both isospin 1 and isospin 0 nucleon states, whereas in the  $pp \rightarrow d\pi^+$  reaction the pn final state has isospin 0. Study of the  $pp \rightarrow pn\pi^+$  reaction over

a kinematic region encompassing the np final state interactions should provide some insight into such questions. The suppression of absorption on isovector nucleon pairs can be understood qualitatively if it is assumed that absorption is dominated by the formation of an  $N\Delta$  intermediate  $s$  state. Such absorption is dominant for an initial isoscalar nucleon pair, but is forbidden for an isovector nucleon pair. If the absorption is not dominated by intermediate  $N\Delta$  formation, many more  $J^{\pi T}$  channels are open. Consequently, at the energies and kinematic conditions appropriate to the present experiment, where pion partial waves of 0 to 2 (with respect to the np system) are important, one might expect both spin singlet and spin triplet final nucleon states to contribute. Such measurements should help cast some light on the extent to which non-isobar channels contribute to the  $pp \rightarrow pn\pi^+$  reaction.

An understanding of the fundamental  $NN \rightarrow NN\pi$  reactions is clearly a prerequisite to an understanding of the more complex phenomena involving pion absorption and production on nuclei. The former reactions constitute the relevant subprocesses involved in the latter reactions, modified by the nuclear environment and by distortions. A simple model of this kind has been used to interpret the  ${}^{12}\text{C}(p, \pi^+)X$  continuum cross sections and analyzing powers<sup>11</sup> in the kinematic regime where the quasifree  $NN \rightarrow NN\pi$  processes should dominate. Both the analyzing powers and the differential cross sections for the  ${}^{12}\text{C}(p, \pi^+)X$  reaction are well described by the model.

### II. EXPERIMENTAL PROCEDURE

#### A. Detection efficiency and spectrometer solid angle

The data presented in this paper were recorded during detailed  $pp \rightarrow d\pi^+$  calibration measurements of a 65 cm

Browne-Buechner magnetic spectrometer, used for a program of nuclear pion production measurements at TRIUMF. These calibration measurements were performed using a  $\text{CH}_2$  target. Each measurement on the  $\text{CH}_2$  target (areal density:  $149 \text{ mg/cm}^2$ ) was followed by a measurement on a carbon target (areal density:  $162 \text{ mg/cm}^2$ ) under identical beam and spectrometer conditions.

The spectrometer system, shown in Fig. 1, incorporated three helically-wound multiwire proportional chambers (MWPC's) for the track reconstruction needed for pion momentum definition. A fast threefold coincidence of scintillation counters ( $\text{CE C1 C2}$ ) was used for definition of the event trigger. Identification of the pion events was made on the basis of energy loss, time of flight, and track reconstruction. The performance of this system has been described in detail by Ziegler.<sup>12</sup> The line shape of a monoenergetic group of pions was determined using pions from the  $\text{pp} \rightarrow \text{d}\pi^+$  reaction measured in coincidence with the associated deuteron. The response function of the system exhibits a significant low energy tail, as well as a smaller high energy tail. These tails arise from multiple scattering of the pions from the magnet pole faces. This phenomenon was exacerbated by the lack of axial focusing in the spectrometer. The fraction of the events which survived the various software cuts was about 0.63 for events in the  $\text{pp} \rightarrow \text{d}\pi^+$  peak, and about 0.15 for events in the tails of the peak (the multiply-scattered events). A parametrization of this survival probability as a function of focal plane position and magnetic field setting was made over the full range of values associated with the measurements reported in this paper.

The effective solid angle of the spectrometer was determined from the measured yields for the  $\text{pp} \rightarrow \text{d}\pi^+$  reaction, corrected for software cuts and wire chamber efficiencies. The effective solid angle, representing the product of the geometrical solid angle multiplied by the pion survival probability, measured at the center of the focal plane, varied from about 2.2 msr at 100 MeV to 1.6 msr

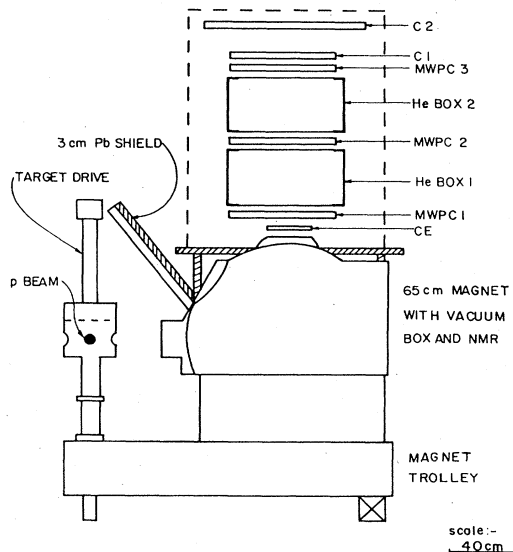


FIG. 1. Pion spectrometer system.

at 30 MeV pion energy. Relative uncertainties in these values are  $\pm 5\%$ , with absolute uncertainties of  $\pm 10\%$ . Dependence of the solid angle on focal plane position was mapped by varying the magnetic field over the range of acceptance of the spectrometer. The input data on the  $\text{pp} \rightarrow \text{d}\pi^+$  reaction required for this calibration included the total cross sections of Richard-Serre *et al.*<sup>13</sup> (350–500 MeV), the compilation of Jones<sup>14</sup> at 400 MeV, and the parametrization of VerWest and Arndt<sup>15</sup> at 450 MeV. The values so obtained are in good agreement with the more recently measured results of Giles *et al.*<sup>16</sup> The angular dependence of the differential cross section for the  $\text{pp} \rightarrow \text{d}\pi^+$  reaction was determined from parameters given in Ref. 14.

### B. Beam normalization and polarization

Simultaneous measurement of the polarization and intensity of the proton beam was accomplished using elastic p-p scattering in a four-arm eight-counter polarimeter<sup>17,18</sup> that detected both the scattered and recoil protons. The analyzing power of the polarimeter was 0.34 and 0.35 at 400 MeV and 450 MeV, respectively. Typical beam polarizations were 66% with intensities of 1–2 nA.

## III. EXPERIMENTAL RESULTS

### A. Spectra and background subtraction

A pion spectrum recorded at 450 MeV proton bombarding energy and at an angle of  $46^\circ$  (lab), using a  $\text{CH}_2$  target, is shown in Fig. 2(a). This spectrum exhibits the  $\text{pp} \rightarrow \text{d}\pi^+$  peak sitting on a large continuum which arises from the  $^{12}\text{C}(p, \pi^+)X$  and  $\text{pp} \rightarrow \text{pn}\pi^+$  reactions. In order to extract the  $\text{pp} \rightarrow \text{pn}\pi^+$  component as carefully as possible, the following procedure was adopted. First of all, the tails of the  $\text{pp} \rightarrow \text{d}\pi^+$  peak were calculated and subtracted from the spectrum. A carbon continuum spectrum, recorded in a separate measurement, was then matched to the region on the high energy side of the  $\text{pp} \rightarrow \text{d}\pi^+$  peak and subtracted. Figure 2(b) shows the resulting spectrum of  $\text{pp} \rightarrow \text{pn}\pi^+$  events. This portion of the spectrum is plotted on an expanded scale in Fig. 2(c), where the small low energy tail of the  $\text{pp} \rightarrow \text{d}\pi^+$  peak is also shown for comparison. A final calculation in which a Gaussian was fitted to the  $\text{pp} \rightarrow \text{d}\pi^+$  peak [Fig. 2(b)] and then subtracted yielded the net  $\text{pp} \rightarrow \text{pn}\pi^+$  spectrum.

### B. Calculation of cross sections and analyzing powers

The net yield  $Y$ , corrected for the software cuts and wire chamber efficiencies as described in Sec. II A, is related to the double differential cross section by the expression

$$Y = n_p n_t \Delta T_\pi \Delta \Omega_{\text{eff}} (d^2\sigma / d^2\Omega dT_\pi), \quad (1)$$

where  $n_p$  is the number of incident protons,  $n_t$  the number of target nuclei per  $\text{cm}^2$ ,  $\Delta T_\pi$  the energy interval, and  $\Delta \Omega_{\text{eff}}$  the effective spectrometer solid angle corrected for focal plane position. Denoting for the moment the double

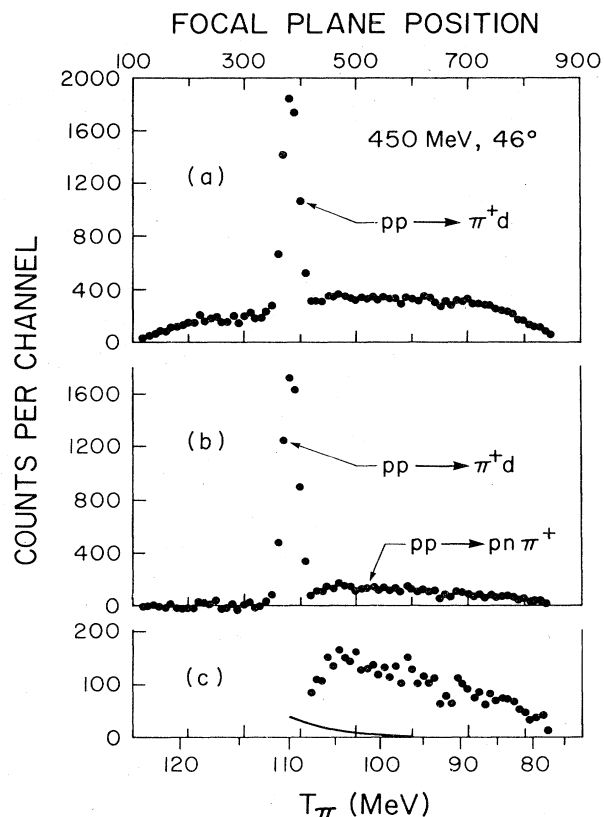


FIG. 2. (a) Pion spectrum from a  $\text{CH}_2$  target recorded at  $46^\circ$  (lab) at a proton bombarding energy of 450 MeV. The continuum to the left of the  $pp \rightarrow d\pi^+$  peak arises from the carbon in the target; that to the right, from carbon and the  $pp \rightarrow pn\pi^+$  reaction. (b) Spectrum after subtraction of the tails on the peak response function and subtraction of the carbon background. (c) Low energy region of (b) on an expanded scale. The solid line shows the magnitude of the low energy tail subtracted.

differential cross section for spin up and spin down by  $\sigma^+$  and  $\sigma^-$ , respectively, the spin averaged cross section is then

$$d^2\sigma(\theta, T_\pi)/d\Omega dT_\pi = \frac{P^-\sigma^+ + P^+\sigma^-}{P^- + P^+}, \quad (2)$$

where  $P^+$  and  $P^-$  are the beam polarizations for spin up and spin down, respectively, defined according to the Madison convention.<sup>19</sup> The analyzing power is given by

$$A_N(\theta, T_\pi) = \frac{\sigma^+ - \sigma^-}{P^+\sigma^- + P^-\sigma^+}. \quad (3)$$

Numerous measurements, corresponding to different magnetic field settings for the spectrometer, were made at each angle for each of the beam energies of 400 and 450 MeV. Comparison of individual measurements at different field settings confirmed the internal consistency of the various calibrations and cut efficiencies, as shown in Fig. 3. In this figure results from four separate measurements, with the  $pp \rightarrow d\pi^+$  peak position spanning a large portion of the useful focal plane range, are displayed.

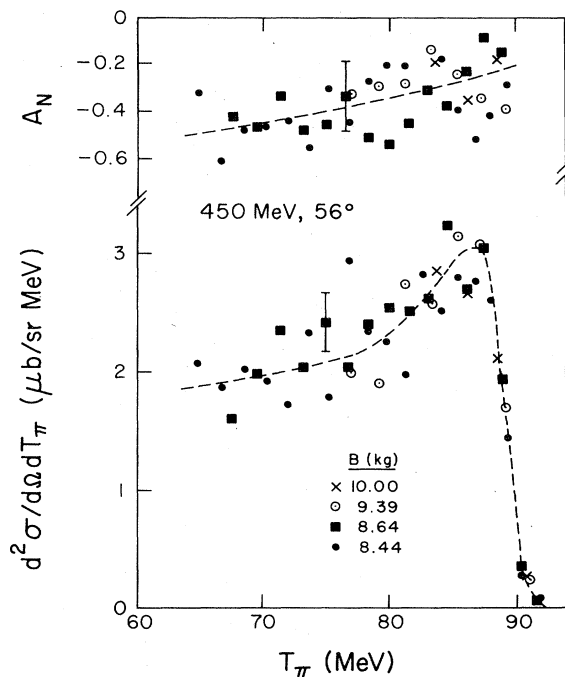


FIG. 3. Cross sections and analyzing powers of the  $pp \rightarrow pn\pi^+$  reaction at 450 MeV and  $46^\circ$ , comparing individual measurements at different magnetic field settings. All quantities are in the laboratory frame. Typical error bars are indicated.

Energy-averaging intervals varied from about 1 MeV at the lowest pion energies to 4 MeV at the highest pion energies.

### C. Results

Results from each angle setting, as illustrated by the data of Fig. 3, were further averaged over several adjacent data points to produce the cross sections and analyzing powers presented in Figs. 4 and 5. One further correction was first applied, however, in order to correct the slight distortion of the shape of the spectrum which arises from the tails of the response function of the system. Since both the tails and the  $pp \rightarrow pn\pi^+$  energy spectra can be approximately represented by an exponential energy dependence, a deconvolution of the data was readily performed. The effect of this deconvolution was small, as can be judged from a comparison of Fig. 3 and the appropriate plot of Fig. 5.

The final results for the analyzing powers and the deconvoluted differential cross sections are shown in Figs. 4 and 5. The differential cross sections show no marked angular dependence. Typical peak values of 2 and 3  $\mu\text{b}/(\text{sr MeV})$  at 400 MeV and 450 MeV energy, respectively, are obtained. However, for all angles a strong enhancement in the cross section is evident at low  $np$  relative energy. A rough extrapolation of the pion energy distributions on a semilogarithmic plot to zero kinetic energy yielded integrated differential cross sections which were

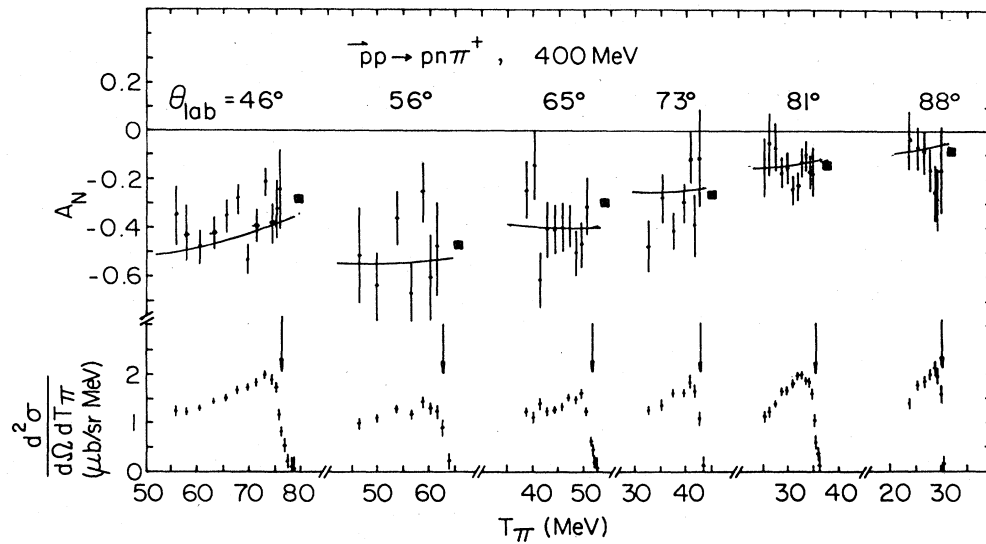


FIG. 4. Cross sections and analyzing powers of the  $pp \rightarrow pn\pi^+$  reaction at 400 MeV as a function of the pion kinetic energy. All quantities are in the laboratory frame. Vertical arrows indicate the pion threshold energies for the  $pp \rightarrow pn\pi^+$  reaction. The solid curves for the analyzing powers have been calculated as discussed in the text. Experimental values of the  $pp \rightarrow d\pi^+$  analyzing powers at the corresponding angles are indicated by the filled squares. Statistical errors only are indicated on the data points.

essentially equal to the  $pp \rightarrow d\pi^+$  differential cross sections at the corresponding bombarding energies. The uncertainties in these cross sections, as a result of the extrapolation, precluded more detailed interpretation of the energy-integrated cross sections.

The analyzing powers are considerably more negative than those of the  $pp \rightarrow d\pi^+$  reaction at the corresponding angles. Furthermore, a marked energy dependence of this analyzing power is observed at 450 MeV, the energy where the statistical uncertainties in the data are smallest. The solid curves shown for the analyzing powers were calculated as described in the following section.

#### IV. DISCUSSION AND CONCLUSIONS

An attempt was made to fit the pion energy spectra with three-body  $pn\pi^+$  final state phase space distributions. Singlet and triplet final state interactions were included in the calculations.<sup>2</sup> Although the results were consistent with a 3:1 statistical mixture of triplet and singlet states, the statistical errors precluded any definitive statement of this ratio.

A further attempt at interpreting the data was made by comparing the measured analyzing powers with those of the  $pp \rightarrow d\pi^+$  reaction. From the measured pion momen-

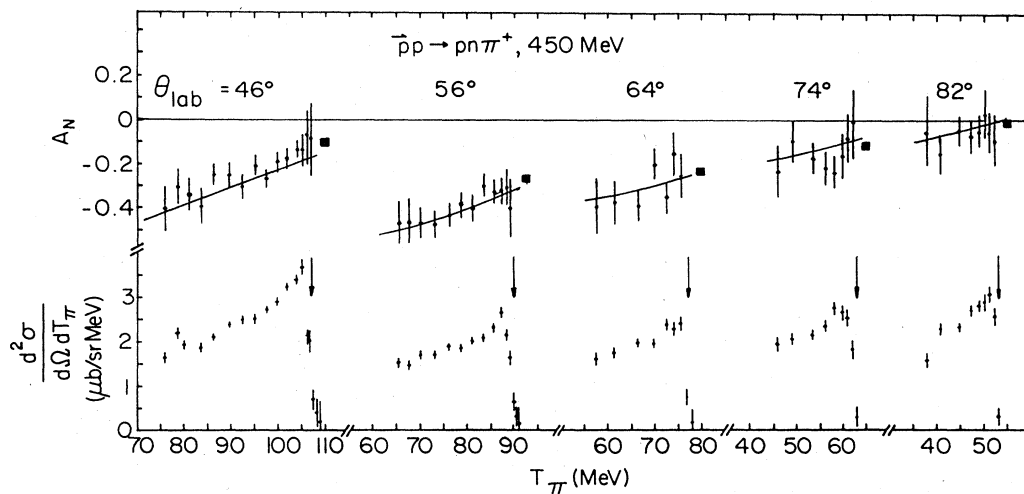


FIG. 5. Cross sections and analyzing powers of the  $pp \rightarrow pn\pi^+$  reaction at 450 MeV as a function of the pion kinetic energy. The rest of the details are as given in Fig. 4.

tum (lab), the center of mass pion momentum and scattering angle are defined through energy and momentum conservation. The  $pp \rightarrow d\pi^+$  analyzing power was calculated at these center of mass values, with the results shown by the solid lines in Figs. 4 and 5. Excellent agreement with the experimental analyzing powers is observed, suggesting that the same spin dependence characterizes both reactions at these kinematical conditions. It should also be noted that the experimental analyzing powers at zero np relative energy are consistent at all angles with the  $pp \rightarrow d\pi^+$  experimental analyzing powers (shown in Figs. 4 and 5 as solid squares). Such observations suggest that the  $pp \rightarrow pn\pi^+$  reaction proceeds primarily through the spin triplet pn channel. This is consistent with the isoscalar dominance observed in the pion absorption experiments.<sup>8-10</sup> However, it must be borne in mind that there is no *a priori* reason why spin singlet and spin triplet NN final states could not exhibit similar features in the analyzing powers, although the different structure of the  $\Delta$  intermediate states accessible<sup>2</sup> would suggest other-

wise. Clearly, further investigations involving higher statistical accuracy are required in order to yield a more definitive statement of the relative importance of the  $S=0$  and  $S=1$  NN final states in the  $pp \rightarrow pn\pi^+$  reaction. In particular, measurements of the FSI region corresponding to low pion energies, where the number of pion partial waves is severely restricted, are very much needed.

*Note added in proof.* The authors would like to note the following early experiments on  $pp \rightarrow pn\pi^+$  asymmetry measurements which were not mentioned in the main text: R. H. March, *Phys. Rev.* **120**, 1874 (1960); R. L. McIlwain *et al.*, *ibid.* **127**, 239 (1962); and A. A. Borisov *et al.*, *Yad Fiz.* **5**, 348 (1967) [*Sov. J. Nucl. Phys.* **5**, 244 (1967)].

#### ACKNOWLEDGMENTS

The extensive assistance of D. Sample in the data analysis is gratefully acknowledged. This work was supported in part by the Natural Sciences and Engineering Research Council of Canada.

\*Present address: Department of Physics and Astronomy, University of Regina, Regina, Saskatchewan, Canada.

<sup>1</sup>G. L. Giles, G. Auld, G. Jones, G. J. Lolos, B. J. McParland, W. Ziegler, D. Ottewell, P. Walden, and W. R. Falk, *Phys. Rev. C* **28**, 2551 (1983); W. R. Falk, E. G. Auld, G. Giles, G. Jones, G. J. Lolos, P. Walden, and W. Ziegler, *ibid.* **25**, 2104 (1982).

<sup>2</sup>G. Jones, *Nucl. Phys.* **A416**, 157c (1984).

<sup>3</sup>B. Blankleider and I. R. Afnan, *Phys. Rev. C* **31**, 1380 (1985); D. V. Bugg, *J. Phys. G* **10**, 717 (1984); M. Betz, B. Blankleider, J. A. Niskanen, and A. W. Thomas, in *Pion Production and Absorption in Nuclei—1981 (Indiana University Cyclotron Facility)*, Proceedings of the Conference on Pion Production and Absorption in Nuclei, AIP Conf. Proc. No. 79, edited by R. D. Bent (AIP, New York, 1982), p. 65.

<sup>4</sup>R. Shypit, C. E. Waltham, D. A. Axen, F. Entezami, M. Comyn, D. Healy, G. A. Ludgate, G. D. Wait, D. V. Bugg, J. A. Edgington, and N. R. Stevenson, *Phys. Lett.* **124B**, 314 (1983).

<sup>5</sup>A. D. Hancock, R. W. Hackenburg, E. V. Hungerford, B. W. Mayes, L. S. Pinsky, J. C. Allred, T. M. Williams, S. D. Baker, J. A. Buchanan, J. M. Clement, M. Copel, I. M. Duck, G. S. Mutchler, G. P. Pepin, E. A. Umland, G. C. Phillips, M. W. McNaughton, C. Huang, and M. Furić, *Phys. Rev. C* **27**, 2742 (1983).

<sup>6</sup>T. S. Bhatia, J. G. J. Boissevain, J. J. Jarmer, R. R. Silbar, J. E. Simmons, G. Glass, J. C. Hiebert, R. A. Kenefick, L. C. Northcliffe, W. B. Tippens, W. M. Kloet, and J. Dubach, *Phys. Rev. C* **28**, 2071 (1983).

<sup>7</sup>J. Hudomalj-Gabitzsch, I. M. Duck, M. Furić, G. S. Mutchler, J. M. Clement, R. D. Felder, W. H. Dragoset, G. C. Phillips, J. C. Allred, E. V. Hungerford, B. W. Mayes, L. S. Pinsky, and T. M. Williams, *Phys. Rev. C* **18**, 2666 (1978).

<sup>8</sup>D. Ashery, R. J. Holt, H. E. Jackson, J. P. Schiffer, J. R. Specht, K. E. Stephenson, R. D. McKeown, J. Ungar, R. McKeown, E. Segel, and P. Zupranski, *Phys. Rev. Lett.* **47**, 895 (1981).

<sup>9</sup>P. Gotta *et al.*, *Phys. Lett.* **112B**, 129 (1982).

<sup>10</sup>G. Backenstoss, M. Izzychi, M. Steinacher, P. Weber, H.-J. Meyer, K. von Weymarn, S. Cierjacks, S. Ljungfelt, U. Man-kin, T. Petkovic, G. Schmidt, H. Ulrich, and M. Furić, *Phys. Lett.* **137B**, 329 (1984).

<sup>11</sup>W. R. Falk, E. G. Auld, G. Giles, G. Jones, G. J. Lolos, W. Ziegler, and P. Walden (unpublished).

<sup>12</sup>W. A. Ziegler, M. S. thesis, University of British Columbia, 1983 (unpublished).

<sup>13</sup>C. Richard-Serre, W. Hirt, D. F. Measday, E. G. Michaelis, M. J. M. Saltmarsh, and P. Skarek, *Nucl. Phys.* **B20**, 413 (1970).

<sup>14</sup>G. Jones, in *Pion Production and Absorption in Nuclei—1981 (Indiana University Cyclotron Facility)*, Proceedings of the Conference on Pion Production and Absorption in Nuclei, AIP Conf. Proc. No. 79, edited by R. D. Bent (AIP, New York, 1982), p. 15.

<sup>15</sup>B. J. VerWest and R. A. Arndt, *Phys. Rev. C* **25**, 1979 (1982).

<sup>16</sup>G. L. Giles, Ph.D. thesis, University of British Columbia, 1985 (unpublished).

<sup>17</sup>E. L. Mathie, Ph.D. thesis, University of British Columbia, 1980 (unpublished).

<sup>18</sup>D. V. Bugg, J. A. Edgington, C. Amsler, R. C. Brown, C. J. Oram, K. Shakarchi, N. M. Stewart, G. A. Ludgate, A. S. Clough, D. Axen, S. Jaccard, and J. Varra, *J. Phys. G* **4**, 1025 (1978).

<sup>19</sup>*Polarization Phenomena in Nuclear Reactions*, edited by H. H. Barschall and W. Haerberli (The University of Wisconsin Press, Madison, 1970), p. xxv.